Steady state multiplicity of two-step biological conversion systems with general kinetics

E.I.P. Volcke[a,b,*], M. Sbarciog[c], E.J.L. Noldus[c], B. De Baets[b], M. Loccufier[c]

[a] *Department of Biosystems Engineering, Ghent University, Coupure links 653, B-9000 Gent, Belgium*
[b] *Department of Applied Mathematics, Biometrics and Process Control, Ghent University, Coupure links 653, B-9000 Gent, Belgium*
[c] *Department of Electrical Energy, Systems and Automation, Ghent University, Technologiepark 913, B-9052 Zwijnaarde, Belgium*

Abstract

This study analyses the steady state behaviour of biological conversion systems with general kinetics, in which two consecutive reactions are carried out by two groups of micro-organisms. The model considered is a realistic description of wastewater treatment processes. A step-wise procedure is followed to reveal the mechanisms affecting the occurrence of steady states in terms of the process input variables. It is clearly demonstrated how taking into account inhibition effects by simply including additional inhibition terms to the kinetic expressions, a common practice, influences the model's long term behaviour. The overall steady state behaviour of the model has been summarized in easy-to-interpret operating diagrams, depicting the occurrence of steady states in terms of the reactor dilution rate and the influent substrate concentration, with well-defined boundaries between distinct

*Corresponding author. Tel.: +32 9 264 61 29; fax: +32 9 264 62 35
Email addresses: eveline.volcke@ugent.be (E.I.P. Volcke), mihaela@autoctrl.ugent.be (M. Sbarciog), erik.noldus@ugent.be (E.J.L. Noldus), bernard.debaets@ugent.be (B. De Baets), mia.loccufier@ugent.be (M. Loccufier)

operating regions. This knowledge is crucial for modelers as steady state multiplicity - in the sense that more than one steady state can be reached depending on the initial conditions - may remain undetected during simulation. The obtained results may also serve for experimental design and for model validation based on experimental findings.
Keywords: Mathematical modeling, Microbial kinetics, Nonlinear dynamics, Stability analysis, Wastewater treatment
2000 MSC: 37N25, 37C10, 34C23, 93D20

1. Introduction

The steady state behaviour of biological conversion systems is an important aspect in view of their process design and control. In particular, process conditions under which steady state multiplicity occurs should be identified accurately. Steady state multiplicity implies that different initial reactor conditions result in different steady states reached for the same choice of input variables. Agrawal et al. [1] formulated conditions under which steady state multiplicity occurs for isothermal continuous stirred bioreactors. Whereas in a non-isothermal reaction system, the nonlinear dependence of the rate constant on temperature may contribute to steady state multiplicity, in isothermal systems like biological wastewater treatment systems, this multiplicity may result from nonlinear kinetics [17]. A widespread application in this field is the nitrification process, i.e. the oxidation of ammonium, being the main form in which nitrogen is present in wastewater. Nitrification can be seen as a two-step reaction, in which a substrate (ammonium) is converted to an intermediate (nitrite), which is subsequently transformed into a final

product (nitrate). The two subsequent conversion reactions are mediated by different groups of microbial species. Accumulation of the intermediate is desirable for innovative nitrogen removal processes based on the nitrite route (see, for example [18]).

The two groups of micro-organisms involved in the two-step conversion system can be termed as commensalistic species, in the sense that the second population benefits from the presence of the first one, which provides the intermediate as the main substrate for the second group, while the first population is unaffected by the presence of the second one. In case the growth of the first population is inhibited by the intermediate, it even benefits from the presence of the second group as the latter removes this inhibiting compound - in this case the relationship between the two populations could even be termed as mutualism (where both organisms benefit). This type of interactions is different from competition between species, where the growth of one species negatively affects the growth of the other one. The steady state and dynamic analysis of various microbial interaction patterns in chemostat reactors, besides other reactor types, has formed the subject of a large number of previous research studies (see e.g. [16], for an analysis of microbial competition in chemostat reactors). To avoid confusion, it is important to stress that the present study deals with two-step biological conversion systems, describing two biomass populations involved in consecutive reactions rather than competition.

The effects of substrate inhibition kinetics for a two-species commensalistic system were studied by Sheintuch [12]. Sheintuch et al. [13] experimentally demonstrated steady state multiplicity in a nitrification reactor with

biomass recycle and presented a kinetic model with substrate inhibition of the second step to describe this behaviour. Volcke et al. [19] demonstrated how microbial (inhibition) kinetics affect the number and the stability of a two-step nitrification model by considering a few different cases w.r.t. the associated reaction kinetics. Anaerobic digestion is another widely applied wastewater treatment process that can be described as a two-step conversion system [3]. During this process, which takes place in absence of oxygen, acidogenic bacteria consume organic substrate and produce volatile fatty acids (VFA), which methanogenic bacteria subsequently convert to methane gas. The latter reaction is inhibited by the intermediate VFA. The stability characteristics of an anaerobic wastewater treatment process have been studied by Hess and Bernard [8] resulting in a criterion to detect the conditions of process destabilisation, characterized by VFA accumulation. A two-step anaerobic digestion model with VFA as an intermediate, extended with gas-liquid transfer and pH effects has been analysed by Shen et al. [14]. In the recent search for new sources of renewable energy, controlling anaerobic digestion towards the production of hydrogen, another process intermediate, is gaining a lot of attention [6]. Hajji et al. [7] addressed the stability of a two-step anaerobic digestion model with hydrogen as an intermediate. In the latter model, the first reaction is characterized by product inhibition, while the second reaction is not influenced by inhibition effects. Noteworthy is that accumulation of the intermediate is highly desirable in certain nitrification reactors and in anaerobic digesters aiming at the production of the intermediate hydrogen, but that accumulation of the intermediate VFA should be absolutely avoided during anaerobic digestion.

From the above, it is clear that several wastewater treatment processes can be described as two-step conversion processes, while the corresponding kinetic expressions vary between different applications. From this perspective, this study focuses on a generic methodology to analyse the correspondence between general reaction kinetics and steady state behavior for two-step biological conversion systems. Inhibition terms, besides substrate limitation terms, are included step by step, to understand thoroughly the impact of multiple inhibition terms on the steady state behaviour. Kinetic expressions with increasing complexity are analysed in a specific order such that the knowledge of the simple models can be transferred to the more complex models. This step-wise analysis is not only advantageous from a mathematical point of view, but also leads to increased insight in the way reaction kinetics affect steady state multiplicity. The results cover a variety of kinetic expressions found in literature and offer an easy to interpret methodology in the form of operating diagrams such that the occurrence of multiple steady states can be recognized for the application under consideration without performing complicated calculations.

2. Bioreactor model

2.1. Two-step conversion model with general kinetics - elementary submodels

The system under study concerns a continuous stirred tank reactor (CSTR) with constant volume, in which two reactions take place, according to the following stoichiometry

$$\begin{aligned} a\,x_1 &\rightarrow c\,x_2 + x_3 \\ b\,x_1 + d\,x_2 &\rightarrow P + x_4 \end{aligned} \tag{1}$$

These reactions are essentially sequential: a substrate x_1 is converted to an intermediate x_2, which is subsequently converted to a final product P. The amount of x_1 consumed in the second reaction is typically small. The two biomass populations x_3 and x_4, which carry out the respective reactions and benefit from this through growth, should therefore in the first place not be seen as competitors (for the same substrate), but as two populations involved in consecutive reactions.

The reaction scheme can describe a two-step nitrification process [19], in which ammonium (x_1) is converted to nitrite (x_2) by ammonium oxidizing biomass (x_3) and subsequently to nitrate (P) by nitrite oxidizing biomass (x_4), using a small amount of ammonium for incorporation in biomass. In a (simplified) two-step anaerobic digestion model [3], x_1 represents organic substrate, which is consumed by acidogens (x_3) to VFA (x_2), which methanogens (x_4) subsequently convert to methane gas (P). In an alternative two-step anaerobic digestion model [7], VFA (x_1) is converted to hydrogen (x_2) by acetogens (x_3), while hydrogen is further converted to methane (P) by methanogens (x_4). In both two-step anaerobic digestion models, the second reaction does not involve x_1, thus $b = 0$ in these applications.

Assuming a constant temperature and pH, the system's state equations are given by the individual mass balances for the components x_i ($i = 1, \ldots, 4$):

$$\begin{aligned} \dot{x}_1 &= u_0\,(u_1 - x_1) - a\,\rho_1(\mathbf{x}) - b\,\rho_2(\mathbf{x}) \\ \dot{x}_2 &= -u_0\,x_2 + c\,\rho_1(\mathbf{x}) - d\,\rho_2(\mathbf{x}) \\ \dot{x}_3 &= -u_0\,x_3 + \rho_1(\mathbf{x}) \\ \dot{x}_4 &= -u_0\,x_4 + \rho_2(\mathbf{x}) \end{aligned} \tag{2}$$

u_0 (> 0) represents the dilution rate (i.e. the ratio of the influent flow rate over the reactor volume), u_1 (> 0) represents the substrate concentration in the influent. It has been assumed that the influent does not contain intermediate, neither biomass. The reaction rates $\rho_i(\mathbf{x})\,(i = 1, 2)$ for the biological conversions (1) are described by

$$\rho_1(\mathbf{x}) = \mu_1(x_1, x_2)\, x_3 \tag{3}$$

$$\rho_2(\mathbf{x}) = \mu_2(x_1, x_2)\, x_4 \tag{4}$$

in which

$$\mu_1(x_1, x_2) \triangleq a_1 \frac{x_1}{b_1 + x_1} \frac{c_1}{c_1 + x_2} \frac{d_1}{d_1 + x_1} \tag{5}$$

$$\mu_2(x_1, x_2) \triangleq \begin{cases} a_2 \dfrac{x_2}{b_2 + x_2} \dfrac{c_2}{c_2 + x_1} \dfrac{d_2}{d_2 + x_2} & \text{if } x_1 > 0 \\ 0 & \text{if } x_1 = 0 \end{cases} \tag{6}$$

The reaction rates $\rho_i,\ i = 1, 2$, depend on the reactor concentrations of the components and consist of substrate limitation terms described as Monod kinetics (in b_i) and inhibition terms (in c_i and d_i). Note that the combination of substrate limitation terms (in b_i) and self-inhibition terms (in d_i) is largely equivalent to the so-called Haldane kinetics. (5) and (6) represent general kinetic expressions, considering all inhibition terms commonly encountered. Setting $\mu_2(x_1, x_2) = 0$ for $x_1 = 0$ to avoid negative reaction rates in case $x_1 = 0$ has been preferred over the alternative of taking up a substrate limitation term in x_1 in (6), in order not to over-complicate the mathematical expressions. With respect to the nitrification process, various kinetic expressions can be found in literature, differing both in the type of inhibitions considered as well as in the values of the corresponding inhibition constants. Some examples have been given by Volcke et al. [19]; an extensive overview

Table 1: Elementary (I-V) and composite (VI-VIII) models considered in this study. c_i and d_i $(i = 1, 2)$ refer to the inhibition terms taken up.

Model	I	II	III	IV	V	VI	VII	VIII
μ_1	-	c_1	d_1	-	-	c_1, d_1	-	c_1, d_1
μ_2	-	-	-	d_2	c_2	-	c_2, d_2	c_2, d_2

has been carried out by Sin et al. [15]. As a rule, these kinetic expressions all consider substrate limitation, but they differ in the number and type of inhibition terms considered - from no inhibition terms to all inhibition terms in (5) and (6). Anaerobic digestion processes are usually described with substrate inhibition of the second reaction as the only inhibition effect (see [3]; [14]), which is described by the term in d_2. Table 1 displays the step-wise addition of inhibition terms, starting from 'elementary' models (models I to V) to end up with 'composite models' (models VI to VIII). c_1, d_1, c_2 and d_2 in Table 1 refer to the corresponding inhibition terms, if not mentioned this means that their value has been assumed to be infinity, i.e. the corresponding inhibition term has not been considered. Model VIII is the most general one and corresponds to the most general kinetic expressions (5) and (6). Table 2 summarizes realistic parameter values for nitrification processes used in the illustrative simulations. The results are generally applicable for other parameter values and to other processes satisfying the stoichiometry and general kinetics given by (1) and (3)-(6), respectively.

Table 2: Numerical parameter values applied in this study (c_2 set arbitrarily, remaining values as in Volcke et al. [19]), as a realistic description of a two-step nitrification process.

Symbol	Value	Unit
a_1	2.1	day^{-1}
b_1	1.32	mole.m^{-3}
c_1	837	mole.m^{-3}
d_1	36	mole.m^{-3}
a_2	1.05	day^{-1}
b_2	0.4	mole.m^{-3}
c_2	125	mole.m^{-3}
d_2	106	mole.m^{-3}

2.2. Canonical state space model representation

The system's state equations in the state variables $\mathbf{x} = \begin{bmatrix} x_1 & x_2 & x_3 & x_4 \end{bmatrix}^T$ are given by the mass balances of the individual components, x_i. They can subsequently be transformed by defining new state space variables $\mathbf{y}$:

$$\mathbf{y} = \begin{bmatrix} y_1 \\ y_2 \\ y_3 \\ y_4 \end{bmatrix} \triangleq \begin{bmatrix} x_1 + a\,x_3 + b\,x_4 \\ x_2 - c\,x_3 + d\,x_4 \\ x_3 \\ x_4 \end{bmatrix} \tag{7}$$

bringing the model in a so-called canonical form [2].

$$\begin{aligned} \dot{y}_1 &= u_0\,(u_1 - y_1) \triangleq g_1(\mathbf{y}) \\ \dot{y}_2 &= -u_0\,y_2 \triangleq g_2(\mathbf{y}) \end{aligned}$$

$$\begin{aligned} \dot{y}_3 &= (-u_0 + \lambda_1(\mathbf{y}))\, y_3 \triangleq g_3(\mathbf{y}) \\ \dot{y}_4 &= (-u_0 + \lambda_2(\mathbf{y}))\, y_4 \triangleq g_4(\mathbf{y}) \end{aligned} \tag{8}$$

in which

$$\lambda_i(\mathbf{y}) = \mu_i(\mathbf{x}) \quad ; \quad i = 1, 2 \tag{9}$$

The canonical model form consists of a linear part of dimension 2 coupled with a nonlinear part of dimension 2. The state variables x_i $(i = 1, \ldots, 4)$ cannot become negative. Call $\mathbf{S_y}$ the image of $\mathbb{R}^{+\,4} \triangleq \{\mathbf{x} \in \mathbb{R}^4 \,|\, x_i \geq 0,\, i = 1, \ldots, 4\}$ under the transformation (7) $\mathbf{x} \mapsto \mathbf{y}$. $\mathbf{S_y}$ is the state space of the system defined by (8). Every trajectory that starts at $t = 0$ in a point $\mathbf{y_0}$ of $\mathbf{S_y}$, stays in $\mathbf{S_y}$ for $t \to +\infty$. It subsequently converges (for positive constant input values u_0 and u_1) to the cross-section Δ of $\mathbf{S_y}$ with the plane $\{y_1 = u_1 \;;\; y_2 = 0\}$. Δ is a bounded region, defined by the inequalities

$$\begin{aligned} u_1 - a\, y_3 - b\, y_4 &\geq 0 \\ c\, y_3 - d\, y_4 &\geq 0 \\ y_3 &\geq 0 \\ y_4 &\geq 0 \end{aligned} \tag{10}$$

The process converges to the second order dynamics (8) with $y_1 = u_1 \;;\; y_2 = 0$. In the sequel, a mathematical steady state solution $\mathbf{y_{ms}}$ of (8) will be called a physical steady state $\mathbf{y_{ss}}$ if it lies in $\mathbf{S_y}$.

3. Multiple steady state behavior

3.1. Calculation of steady states

Using the canonical state space model representation, the calculation of steady states of the model is substantially simplified. For positive dilution

rates ($u_0 > 0$) and influent substrate concentrations ($u_1 > 0$), the steady states are obtained from (8) in which $\dot{y}_i = 0$ ($i = 1, \ldots, 4$):

$$\begin{aligned} y_{ss1} &= u_1 \\ y_{ss2} &= 0 \\ (-u_0 + \lambda_1(\mathbf{y_{ss}}))\ y_{ss3} &= 0 \\ (-u_0 + \lambda_2(\mathbf{y_{ss}}))\ y_{ss4} &= 0 \end{aligned} \tag{11}$$

Note that, at steady state, $\lambda_2(\mathbf{y}) = \mu_2(\mathbf{x}) \neq 0$, so the nontrivial expression in (6) holds, since no steady state exists for which the substrate concentration is zero ($x_{ss1} = 0$), for a given $u_0 > 0$ and $u_1 > 0$. Indeed, $x_{ss1} = 0$ implies that $\lambda_1(\mathbf{y_{ss}}) = \mu_1(\mathbf{x_{ss}}) = 0$ (see (5), (6) and (9)), so $y_{ss3} = y_{ss4} = 0$ (see (11) for $u_0 \neq 0$) and consequently $y_{ss1} = 0$ (see (7)), which requires $u_1 = 0$ (see (11)). From the definition of y_2 (see (7)), given that $y_{ss2} = 0$ and considering the physical boundary conditions $x_2 \geq 0$ and $x_4 \geq 0$, it follows that $x_{ss3} = y_{ss3} = 0$ (no biomass for first reaction) also implies $x_{ss4} = y_{ss4} = 0$ (no biomass for second reaction). Besides, this also results in $x_{ss2} = 0$. This seems logical regarding the fact that the reactions are consecutive and given that the influent does not contain either intermediate or biomass: in the absence of biomass responsible for the first conversion reaction, no intermediate is generated in the reactor, thus the second reaction cannot proceed. The corresponding biomass cannot grow and will be washed out if initially present.

Consequently, three different types of steady states are obtained from (11):

1. $y_{ss3} = y_{ss4} = 0$: the washout state $\mathbf{y_{ss}^W}$- no biomass is present and hence no conversion takes place.

2. $y_{ss4} = 0$; $y_{ss3} \neq 0$: only intermediate (x_2) is produced - this type of steady state is further denoted by $\mathbf{y}_{\mathbf{ss}}^{\alpha}$
3. $y_{ss3} \neq 0$; $y_{ss4} \neq 0$: with formation of product (P) - this type of steady state is further denoted by $\mathbf{y}_{\mathbf{ss}}^{\beta}$

The washout state is unique and is always a physical steady state. Its value is given by

$$\mathbf{x}_{\mathbf{ss}}^{\mathbf{W}} = \begin{bmatrix} u_1 & 0 & 0 & 0 \end{bmatrix}^T \tag{12}$$

In the remaining two cases, the number of steady states depends on the conversion kinetics. The steady states in which only intermediate is produced (type α) are found as

$$\left.\begin{array}{rcl} y_{ss1}^{\alpha} & = & u_1 \\ y_{ss2}^{\alpha} & = & 0 \\ u_0 & = & \lambda_1(\mathbf{y}_{\mathbf{ss}}^{\alpha}) \\ y_{ss4}^{\alpha} & = & 0 \end{array}\right\} \Rightarrow \mathbf{x}_{\mathbf{ss}}^{\alpha} = \begin{bmatrix} x_{ss1}^{\alpha} \\ \dfrac{c}{a}\,(u_1 - x_{ss1}^{\alpha}) \\ \dfrac{1}{a}\,(u_1 - x_{ss1}^{\alpha}) \\ 0 \end{bmatrix} \tag{13}$$

in which x_{ss1}^{α} results from

$$\mu_1^{\alpha} \triangleq \mu_1\left(x_{ss1}^{\alpha}, \frac{c}{a}\,(u_1 - x_{ss1}^{\alpha})\right) = u_0 \tag{14}$$

The steady states corresponding to product formation (type β) are found as

$$\left.\begin{array}{rcl} y_{ss1}^{\alpha} & = & u_1 \\ y_{ss2}^{\alpha} & = & 0 \\ u_0 & = & \lambda_1(\mathbf{y}_{\mathbf{ss}}^{\beta}) \\ u_0 & = & \lambda_2(\mathbf{y}_{\mathbf{ss}}^{\beta}) \end{array}\right\} \Rightarrow \mathbf{x}_{\mathbf{ss}}^{\beta} = \begin{bmatrix} x_{ss1}^{\beta} \\ x_{ss2}^{\beta} \\ \dfrac{d\left(u_1 - x_{ss1}^{\beta}\right) + b\,x_{ss2}^{\beta}}{a\,d + b\,c} \\ \dfrac{c\left(u_1 - x_{ss1}^{\beta}\right) - a\,x_{ss2}^{\beta}}{a\,d + b\,c} \end{bmatrix} \tag{15}$$

with x^{β}_{ss1} and x^{β}_{ss2} calculated from

$$\begin{cases} \mu_1\left(x^{\beta}_{ss1}, x^{\beta}_{ss2}\right) = u_0 \\ \mu_2\left(x^{\beta}_{ss1}, x^{\beta}_{ss2}\right) = u_0 \end{cases} \tag{16}$$

It is clear that the number of solutions of type $\mathbf{x}^{\alpha}_{\mathbf{ss}}$ and $\mathbf{x}^{\beta}_{\mathbf{ss}}$ is not always unique. Besides, one also needs to check rigorously whether the steady states calculated mathematically are actually physical steady states in the sense that they lie in $\mathbf{S_y}$ (in the $\mathbf{y}$-space) or $\mathbb{R}^{+4}$ (in the $\mathbf{x}$-space). It is important to note that, while some solutions of (13)-(14) and (15)-(16) can be excluded a priori from being physical steady states, others being physical steady states or not will depend on the values of the input variables u_0 and u_1. The calculation of steady states and the identification of conditions for physical steady states are assessed in what follows for all models I-VIII.

3.2. Steady states with formation of intermediate only (type α)

The steady states in which only intermediate is formed, corresponding to suppression of the second reaction in (1), are obtained from (13)–(14). It is important to note that only the kinetics $\mu_1(x_1, x_2)$ of the first reaction determines the value of x^{α}_{ss}. According to Table 1, four cases can be defined, which cluster the models with the same steady state multiplicity: model I, IV, V and VII (case 1); model II (case 2); model III (case 3); model VI and VIII (case 4). The number of mathematical solutions x^{α}_{ms1} depends on the expression of the growth kinetics. A mathematical steady state $\mathbf{x}^{\alpha}_{\mathbf{ms}}$ is not necessarily a physical steady state $\mathbf{x}^{\alpha}_{\mathbf{ss}}$ which lies in $\mathbb{R}^{+4}$. From (13), it is clear that a steady state with only intermediate formation, $\mathbf{x}^{\alpha}_{\mathbf{ss}}$, actually

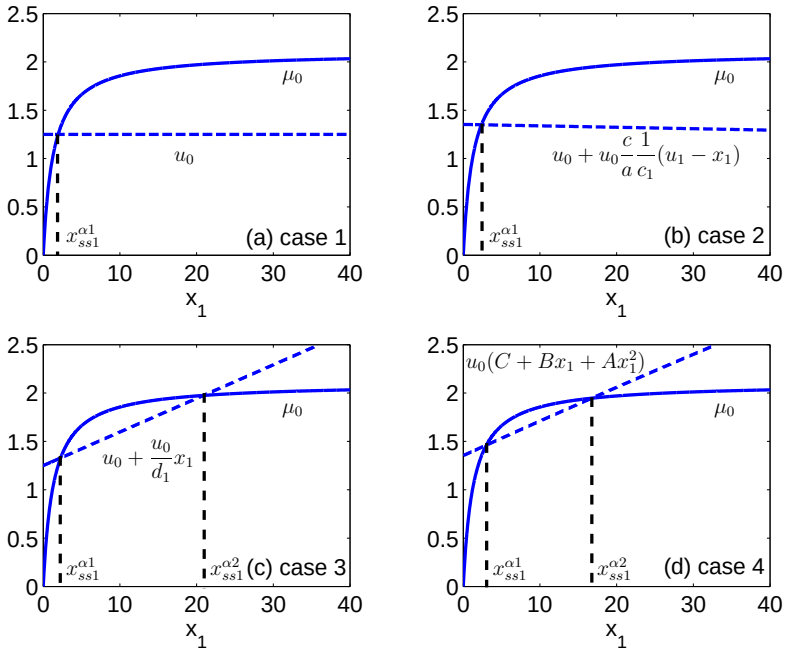

Figure 1: Graphical representation (for $u_0 = 1.25$; $u_1 = 70$) of x_{ss1}^{α} satisfying (14). Subfigures a, b, c and d correspond to case 1 (models I, IV, V, VII), case 2 (model II), case 3 (model III) and case 4 (models VI, VIII), respectively. Note the small negative slope in case 2 and the maximum of the parabola lying very far to the right in case 4, for the given (realistic) parameter values.

occurs (is a physical steady state) under the condition

$$0 < x_{ss1}^{\alpha} < u_1 \tag{17}$$

(17) yields in each case conditions to be satisfied for the input variables u_0 and u_1 w.r.t. the parameters a_1, b_1, c_1, d_1 characterizing $\mu_1(x_1, x_2)$.

In case 1, (14) simplifies to

$$a_1 \frac{x_1}{b_1 + x_1} = u_0 \tag{18}$$

We define

$$\mu_0(x_1) \triangleq a_1 \frac{x_1}{b_1 + x_1}$$

Relationship (18) is the intersection of the Monod type kinetics $\mu_0(x_1)$ with a horizontal line as illustrated in Fig. 1a. There will be a mathematical solution $x_{ms1}^{\alpha_1} = \dfrac{b_1 u_0}{a_1 - u_0}$ if

$$u_0 < \lim_{x_1 \to \infty} \mu_1(x_1) = a_1$$

x_{ms1}^{α} represents a physical state $x_{ss1}^{\alpha_1}$ if $x_{ms}^{\alpha_1} < u_1$ or

$$u_0 < \frac{a_1 u_1}{b_1 + u_1} \tag{19}$$

The solution of case 2 can easily be compared with the one of case 1 if (14) is rewritten as

$$a_1 \frac{x_1}{b_1 + x_1} = u_0 + u_0 \frac{c}{a} \frac{1}{c_1}(u_1 - x_1) \tag{20}$$

We obtain the intersection of the Monod type kinetics $\mu_0(x_1)$ and a straight line with negative slope as depicted in Fig. 1b, yielding again a unique mathematical solution $\mathbf{x_{ms}^{\alpha_2}}$. The right hand side of (20) is larger than u_0 for $0 < x_1 < u_1$ and equals u_0 for $x_1 = u_1$ such that the mathematical solution is a physical solution $x_{ss1}^{\alpha_2} > x_{ss1}^{\alpha_1}$ if (19) is satisfied.

In case 3, (14) is rewritten as:

$$a_1 \frac{x_1}{b_1 + x_1} = u_0 + \frac{u_0}{d_1} x_1 \tag{21}$$

The Monod characteristic $\mu_0(x_1)$ in Fig. 1c is intersected with a straight line starting from u_0 for $x_1 = 0$ and having slope $\dfrac{u_0}{d_1}$. If $u_0 < \dfrac{a_1 u_1}{b_1 + u_1} \dfrac{d_1}{d_1 + u_1}$, one

physical state is obtained. If $u_0 \geq \frac{a_1 u_1}{b_1+u_1}\frac{d_1}{d_1+u_1}$ and $u_0 < \frac{a_1 u_1}{b_1+u_1}$, several possibilities occur, depending on the discriminant of the quadratic equation

$$x_1^2 + \left(b_1 + d_1 - \frac{a_1 d_1}{u_0}\right) x_1 + b_1 d_1 = 0$$

Let

$$D = \sqrt{\left(b_1 + d_1 - \frac{a_1 d_1}{u_0}\right)^2 - 4 b_1 d_1}$$

Then

$$\begin{aligned} D > 0 &\Rightarrow \text{two physical states} \\ D = 0 &\Rightarrow \text{one physical state} \\ D < 0 &\Rightarrow \text{no physical state} \end{aligned}$$

$x_1 > 0$ implies $u_0 < \frac{a_1 d_1}{b_1+d_1}$. Although $D > 0$ implies two options for u_0, only option (22) leads to physical solutions :

$$u_0 < \frac{a_1 d_1}{\left(\sqrt{b_1} + \sqrt{d_1}\right)^2} \tag{22}$$

The flowchart shown in Fig. 2 represents schematically the conditions which lead to physical steady states for case 1, 2 and 3.

The final case, case 4, is the most complicated one. (14) is manipulated as follows:

$$\begin{aligned} a_1 \frac{x_1}{b_1 + x_1} &= u_0 \frac{c_1 + \frac{c}{a}(u_1 - x_1)}{c_1} \frac{d_1 + x_1}{d_1} \\ &= u_0 \left(1 + \frac{c}{a}\frac{1}{c_1} u_1 + \left(\frac{1}{d_1} + \frac{c}{a}\frac{1}{c_1}\frac{1}{d_1} u_1 - \frac{c}{a}\frac{1}{c_1}\right) x_1 - \frac{c}{a}\frac{1}{c_1}\frac{1}{d_1} x_1^2\right) \end{aligned}$$

Define

$$\begin{aligned} A &\triangleq -\frac{c}{a}\frac{1}{c_1}\frac{1}{d_1} \\ B &\triangleq \frac{1}{d_1} + \frac{c}{a}\frac{1}{c_1}\frac{1}{d_1} u_1 - \frac{c}{a}\frac{1}{c_1} \\ C &\triangleq 1 + \frac{c}{a}\frac{1}{c_1} u_1 \end{aligned}$$

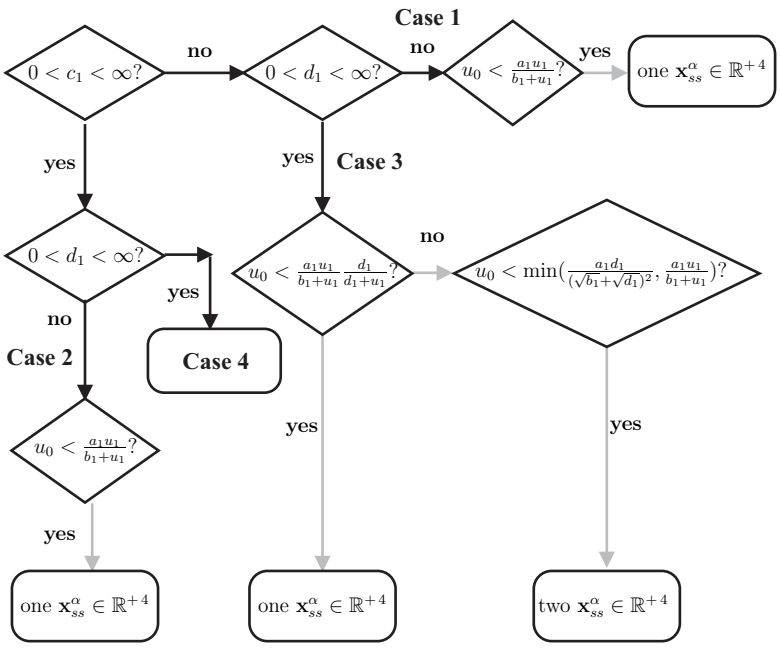

Figure 2: Flowchart with the conditions for physical steady states in case 1 (models I, IV, V, VII), case 2 (model II) and case 3 (model III). Case 4 (models VI, VIII) is detailed in Fig. 3

and

$$F(x_1) \triangleq u_0(C + Bx_1 + Ax_1^2)$$

The mathematical solutions of (14) in case 4 result from the intersection of the Monod type kinetics $\mu_0(x_1)$ and a parabola $F(x_1)$ with a maximum at $x_1 = \dfrac{-B}{2A}$. The x_1 coordinate of the maximum is not influenced by the value of u_0. The value of $F\left(\dfrac{-B}{2A}\right)$ plays an important role in the number of physical steady states. If $\dfrac{-B}{2A} \leq 0$, then only one mathematical solution occurs as $0 < F(0)$. This solution is a physical steady state $x_{ss1}^{\alpha_4}$ if $F(u_1) \leq a_1 \dfrac{u_1}{b_1 + u_1}$. Several situations are distinguished for $\dfrac{-B}{2A} > 0$:

1. $F\left(\frac{-B}{2A}\right) < \frac{a_1 u_1}{b_1 + u_1}$: As $0 < F(0) < F\left(\frac{-B}{2A}\right)$ and $F(x_1)$ increases for $0 < x_1 < \frac{-B}{2A}$, only one mathematical solution is obtained, which is a physical solution $x_{ss1}^{\alpha_4} < u_1$.
2. $F\left(\frac{-B}{2A}\right) > \frac{a_1 u_1}{b_1 + u_1}$: For $0 < x_1 < \frac{-B}{2A}$ two increasing curves $\mu_0(x_1)$ and $F(x_1)$ intersect. Mathematical solutions are found by solving the equation:

$$x_1^2 + \left(b_1 + d_1 - \frac{a_1 d_1}{u_0} \frac{c_1}{c_1 + \frac{c}{a}(u_1 - x_1)} \right) x_1 + b_1 d_1 = 0 \qquad (23)$$

Two mathematical solutions will be found if

$$\left(b_1 + d_1 - \frac{a_1 d_1}{u_0} \frac{c_1}{c_1 + \frac{c}{a}(u_1 - x_1)} \right)^2 - 4 b_1 d_1 > 0$$

or

$$u_0 < \frac{a_1 d_1}{(\sqrt{b_1} + \sqrt{d_1})^2} \frac{c_1}{c_1 + \frac{c}{a}(u_1 - x_1)}$$

A sufficient condition for the existence of two mathematical solutions is:

$$u_0 < \frac{a_1 d_1}{(\sqrt{b_1} + \sqrt{d_1})^2} \frac{c_1}{c_1 + \frac{c}{a} u_1} \qquad (24)$$

There is no solution if

$$u_0 > \frac{a_1 d_1}{(\sqrt{b_1} + \sqrt{d_1})^2} \qquad (25)$$

In case that $\frac{a_1 d_1}{(\sqrt{b_1} + \sqrt{d_1})^2} \frac{c_1}{c_1 + \frac{c}{a} u_1} < u_0 < \frac{a_1 d_1}{(\sqrt{b_1} + \sqrt{d_1})^2}$, a numerical verification is needed to conclude whether two solutions exist for $0 < x_1 < \frac{-B}{2A}$. The mathematical solutions are physical solutions if $0 <$

$\frac{-B}{2A} < u_1$ or $\frac{-B}{2A} > u_1$ and $F(u_1) > \frac{a_1 u_1}{b_1 + u_1}$. If $0 < \frac{-B}{2A} < u_1$ a third physical solution will occur in case $F(u_1) \leq \frac{a_1 u_1}{b_1 + u_1}$.

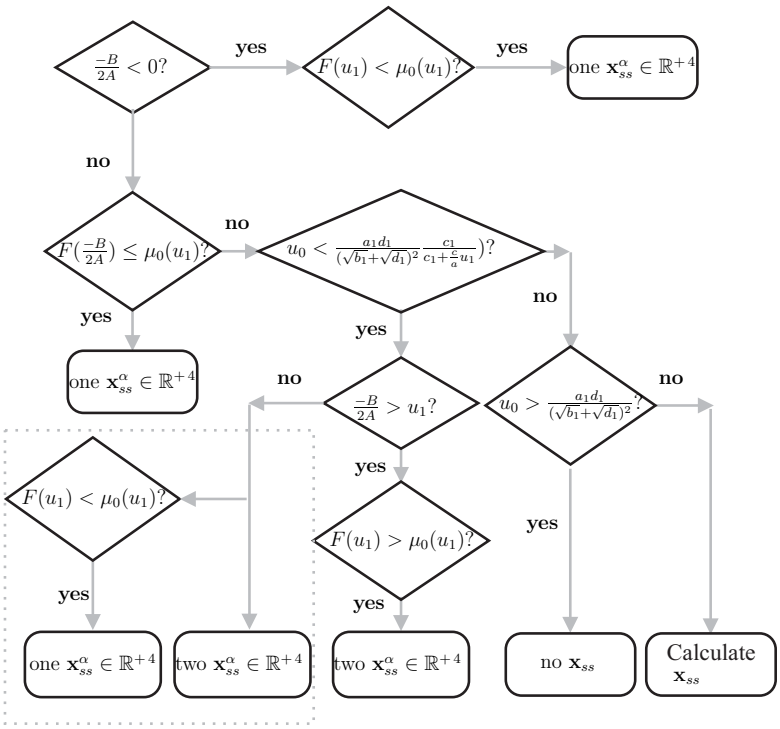

Figure 3: Flowchart with the conditions for physical steady states in case 4 (models VI, VIII)

The flowchart shown in Fig. 3 summarizes the conditions for physical steady states in case 4. The dotted square indicates conditions where three α-type steady states occur. However, the operating diagrams in Section 4.2 will indicate that these conditions are rarely satisfied.

3.3. Steady states with product formation (type β)

The steady states corresponding to product formation, $\mathbf{x}_{\mathbf{ss}}^{\beta}$, are obtained from (15)-(16). The mathematical solutions found in Section 3.2 for case 1

and case 3 can be reused for the β-type steady states of models I to VII. Therefore we define:

$$\Phi(u_0) \triangleq u_0 + \frac{b_2\,(u_0)^2}{c_1\,(a_2 - u_0)} \tag{26}$$

$$\Psi(u_0) \triangleq u_0 + \frac{b_1\,(u_0)^2}{c_2\,(a_1 - u_0)} \tag{27}$$

Table 3 shows the case and corresponding necessary substitutions to reuse the mathematics of Section 3.2. From (15), it is clear that a steady state corresponding to product formation, $\mathbf{x}_{\mathbf{ss}}^{\beta}$, actually occurs (is a physical steady state) under the conditions

$$0 \;<\; x_{ss1}^{\beta} \tag{28}$$

$$0 \;<\; x_{ss2}^{\beta} \tag{29}$$

$$u_1 \;>\; x_{ss1}^{\beta} + \frac{a}{c}\,x_{ss2}^{\beta} \tag{30}$$

Note that u_1 has no influence on the expression the β-type steady states for the models I to VIII as only case 1 and 3 are needed for the calculations. Table 3 clearly shows the duality for the calculations and corresponding conditions between models II and V, models III and IV, models VI and VII.

The β-type steady states of model VIII have the expression (15), where $x_{ss_1}^{\beta,\mathrm{VIII}}$ and $x_{ss_2}^{\beta,\mathrm{VIII}}$ result from the solution of (16). (16) can be rewritten as:

$$\begin{cases} b_1 d_1 + \left(b_1 + d_1 - \dfrac{c_1}{c_1 + x_2}\dfrac{a_1\,d_1}{u_0}\right) x_1 + x_1^2 \;=\; 0 \\ b_2 d_2 + \left(b_2 + d_2 - \dfrac{c_2}{c_2 + x_1}\dfrac{a_2\,d_2}{u_0}\right) x_2 + x_2^2 \;=\; 0 \end{cases} \tag{31}$$

We take a closer look at the expressions of the roots of (31) where $i = 1, 2$ indicates the two roots for x_1 and the two roots for x_2:

$$x_{1_i} \;=\; -\frac{1}{2}\left(b_1 + d_1 - \frac{c_1}{c_1 + x_2}\frac{a_1 d_1}{u_0}\right) \pm$$

Table 3: Overview of the analogy to calculate β-type steady states based on case 1 and 3 for the α-type steady states

Model	Steady states	Case	Substitutions
I	$x_{ss1}^{\beta^1}$	case 1	/
	$x_{ss2}^{\beta^1}$	case 1	$a_1 \rightarrow a_2$
			$b_1 \rightarrow b_2$
II	$x_{ss1}^{\beta^2}$	case 1	$u_0 \rightarrow \Phi(u_0)$
	$x_{ss2}^{\beta^2}$	case 1	$a_1 \rightarrow a_2$
			$b_1 \rightarrow b_2$
III	$x_{ss1}^{\beta^3}$	case 3	/
	$x_{ss2}^{\beta^3}$	case 1	$a_1 \rightarrow a_2$
			$b_1 \rightarrow b_2$
IV	$x_{ss1}^{\beta^4}$	case 1	/
	$x_{ss2}^{\beta^4}$	case 3	$a_1 \rightarrow a_2$
			$b_1 \rightarrow b_2$
			$d_1 \rightarrow d_2$
V	$x_{ss1}^{\beta^5}$	case 1	/
	$x_{ss2}^{\beta^5}$	case 1	$u_0 \rightarrow \Psi(u_0)$
VI	$x_{ss1}^{\beta^6}$	case 3	$u_0 \rightarrow \Phi(u_0)$
	$x_{ss2}^{\beta^6}$	case 1	$a_1 \rightarrow a_2$
			$b_1 \rightarrow b_2$
VII	$x_{ss1}^{\beta^7}$	case 1	/
	$x_{ss2}^{\beta^7}$	case 3	$a_1 \rightarrow a_2$
			$b_1 \rightarrow b_2$
			$c_1 \rightarrow c_2$
			$d_1 \rightarrow d_2$
			$u_0 \rightarrow \Psi(u_0)$

$$\frac{1}{2}\sqrt{\left(b_1+d_1-\frac{c_1}{c_1+x_2})\frac{a_1d_1}{u_0}\right)^2-4b_1d_1} \quad (32)$$

$$x_{2_i} = -\frac{1}{2}\left(b_2+d_2-\frac{c_2}{c_2+x_1}\frac{a_2d_2}{u_0}\right)\pm$$

$$\frac{1}{2}\sqrt{\left(b_2+d_2-\frac{c_2}{c_2+x_1})\frac{a_2d_2}{u_0}\right)^2-4b_2d_2} \quad (33)$$

(32) and (33) are real-valued solutions if respectively:

$$x_2 < \left(\frac{a_1\,d_1}{(\sqrt{b_1}+\sqrt{d_1})^2}\frac{1}{u_0}-1\right)c_1 \quad (34)$$

$$x_1 < \left(\frac{a_2\,d_2}{(\sqrt{b_2}+\sqrt{d_2})^2}\frac{1}{u_0}-1\right)c_2 \quad (35)$$

As $x_2 \geq 0$ and $x_1 \geq 0$, (34) and (35) define an upper limit for the dilution rate u_0:

$$u_0 < \min\left(\frac{a_2\,d_2}{(\sqrt{b_2}+\sqrt{d_2})^2}, \frac{a_1\,d_1}{(\sqrt{b_1}+\sqrt{d_1})^2}\right) \triangleq u_{0max} \quad (36)$$

Any solution of (31) will be a physical solution if the choice of u_1 is such that (28), (29) and (30) are satisfied as well. Based on the nature of equations (31), there can be up to 4 steady states of type β. However, no analytical expressions can be derived for their occurrence in terms of u_0 and u_1. If $u_0 \to 0$ then according to (32) and (33):

$$\begin{aligned}
x_{1_1} &\to 0 \\
x_{1_2} &\to -\left(b_1+d_1-\frac{c_1}{c_1+x_2}\frac{a_1d_1}{u_0}\right) \\
x_{2_1} &\to 0 \\
x_{2_2} &\to -\left(b_2+d_2-\frac{c_2}{c_2+x_1}\frac{a_2d_2}{u_0}\right)
\end{aligned}$$

Based on (30) we can conclude that all mathematical solutions will be phys-

ical solutions if

$$-\left(b_1 + d1 - \frac{a_1 d_1}{u_0}\right) + \frac{a}{c}\left(-\left(b_2 + d_2 - \frac{a_2 d_2}{u_0}\right)\right) < u_1$$

or

$$u_0 > \frac{a_1 d_1 + \frac{a}{c} a_2 d_2}{u_1 + b_1 + d_1 + b_2 + d_2} \tag{37}$$

The latter is of course only a sufficient condition which can be conservative. (32) and (33) indicate the sensitivity of the solutions w.r.t. the dilution rate u_0. The roots (32) and (33) are plotted for two choices of u_0: in Fig. 4 u_0 is chosen close to (36), $u_0 = 0.96 \times u_{0max}$, while in Fig. 5 $u_0 = 0.75 \times u_{0max}$. Relationships (32) and (33) define two branches in the x_1x_2-plane. The mathematical solutions are the intersections of these branches. The mathematical solutions are physical solutions if they lie inside the triangle defined by (28), (29) and (30) in the x_1x_2-plane. In Fig. 4 two physical steady states of type β exist, while in Fig. 5 only one occurs, close to the origin. Due to the large ratio $\frac{c_1}{c_2}$ the branches corresponding to (33) are much smaller than those corresponding to (32).

The steady state behaviour for the individual models is summarized in the following section, considering all type of steady states at the same time and assessing their local stability. The results are translated into operating diagrams, which allow an operator to analyse the steady state multiplicity for a two-step biological process in a very straightforward and easy to interpret manner.

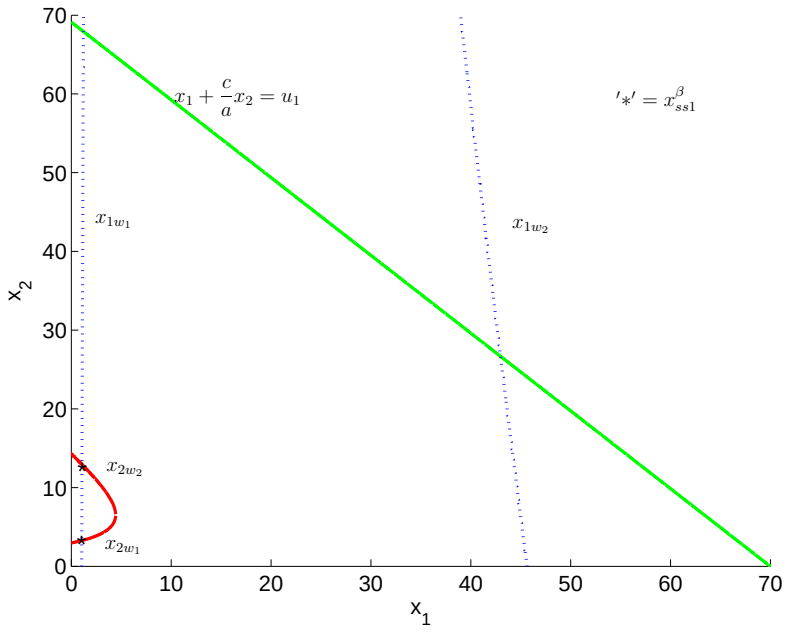

Figure 4: β-type steady states of model VIII for $u_0 = 0.97 \times u_{0max}$, (32) and (33) plotted in the x_1x_2-plane

4. Overall steady state behaviour

4.1. Local stability of steady states

A physical steady state is an operation point if it is locally asymptotically stable (l.a.s.). The linearization principle is used to investigate the local asymptotic stability of steady states. The stability of a steady state $\mathbf{x_{ss}}$ is equivalent to the one of the corresponding $\mathbf{y_{ss}}$ and is assessed using the canonical state space model representation. A steady state $\mathbf{y_{ss}}$ of the system represented by (8) is locally asymptotically stable if all eigenvalues of the system's Jacobian matrix, evaluated for this steady state, $\mathbf{J}(\mathbf{y_{ss}}) = \left.\frac{\partial \mathbf{g}(\mathbf{y})}{\partial \mathbf{y}}\right|_{\mathbf{y}=\mathbf{y_{ss}}}$, possess strictly negative real parts. It can easily be seen that $\mathbf{J}(\mathbf{y_{ss}})$ has a double eigenvalue $-u_0$ and that its remaining two eigenvalues are the eigen-

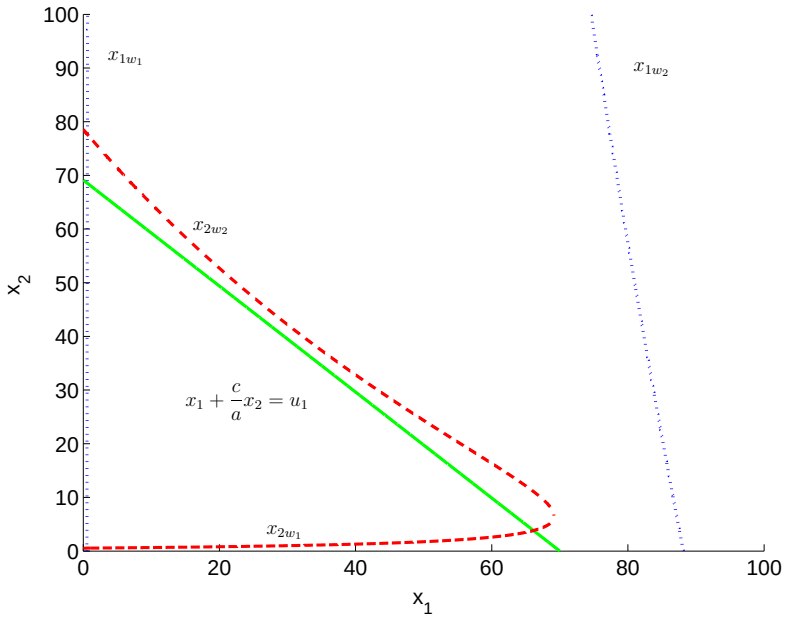

Figure 5: β-type steady states of model VIII for $u_0 = 0.75 \times u_{0max}$, (32) and (33) plotted in the x_1x_2-plane

values of the 2-dimensional matrix

$$\mathbf{J_{34}}(\mathbf{y_{ss}}) = \begin{bmatrix} \left.\frac{\partial\, g_3}{\partial\, y_3}\right|_{\mathbf{y}=\mathbf{y_{ss}}} & \left.\frac{\partial\, g_3}{\partial\, y_4}\right|_{\mathbf{y}=\mathbf{y_{ss}}} \\ \left.\frac{\partial\, g_4}{\partial\, y_3}\right|_{\mathbf{y}=\mathbf{y_{ss}}} & \left.\frac{\partial\, g_4}{\partial\, y_4}\right|_{\mathbf{y}=\mathbf{y_{ss}}} \end{bmatrix} \tag{38}$$

The linearization principle provides a necessary and sufficient condition for local asymptotic stability for so-called hyperbolic steady states, of which the Jacobian matrix has no eigenvalues on the imaginary axis. The results are summarized in Table 4. Detailed calculations can be found in Appendix A.

Aside equilibrium points, the limit set of a two-dimensional system may also contain limit cycles. Corollary 1.8.5 in [5] states that a limit cycle may exist only around a l.a.s. or index 2 equilibrium point, or it may enclose on odd number of equilibria (say $2n + 1$), of which n must be index 1 and

$n+1$ must be either l.a.s. or index 2. According to this corollary, the only possibility for a limit cycle to occur in the physical state space of the two-step biological systems is around the l.a.s. equilibrium point $\mathbf{y}_{\mathbf{ss}}^{\boldsymbol{\beta}\mathbf{1}}$. Let us assume that such a limit cycle γ occurs.

According to the theoretical concepts presented in [4] and the general framework for the stability analysis of biochemical reaction systems developed by Sbarciog [11], there exists a nonempty, nontrivial intersection between the region of attraction of a l.a.s. equilibrium point and the unstable manifold of equilibria lying on the stability boundary of this l.a.s. equilibrium, for systems which satisfy several conditions: i) transversality, ii) hyperbolic equilibrium points, iii) bounded solutions. [11] contains a detailed formulation of these conditions. As the two-step biological system under study satisfies those conditions, intersections of system's trajectories with the limit cycle γ would occur. This is in contradiction with the uniqueness of system's solutions. Thus, no limit cycle can occur on the plane Δ and every system's trajectory converges to an equilibrium point.

As indicated in Table 4, there are many cases when several locally asymptotically stable (l.a.s.) steady states occur for two-step biological processes. In these cases, whether or not the dynamics converge to a l.a.s. steady state or the other depends on the initial condition of the system. The set of initial states which lead the system to a l.a.s. steady state $\mathbf{x}_{\mathbf{ss}}$ is called the region of attraction of $\mathbf{x}_{\mathbf{ss}}$. Having an accurate estimate of the region of attraction [10] plays an important role in the system's operation as not all l.a.s. steady states are technologically meaningful (desirable).

Table 4: Stability characteristics of the steady states ($\mathbf{x_{ss}^W}$: washout; $\mathbf{x_{ss}^\alpha}$: only intermediate formation ; $\mathbf{x_{ss}^\beta}$: product formation) in the different operating zones for all models under study. l.a.s., g.a.s.: locally, globally asymptotically stable. *quasi*: except for some trajectories. For unstable steady states, the index (number of positive eigenvalues) is mentioned between brackets. n.a.: not applicable.

	Model	I, II, V Fig. 6	III	IV,VII Fig. 10	VI Fig. 8
zone W	$\mathbf{x_{ss}^W}$	g.a.s.	g.a.s.	g.a.s.	g.a.s.
zone	$\mathbf{x_{ss}^W}$	unstable (1)	unstable (1)	unstable (1)	unstable (1)
$W\alpha 1$	$\mathbf{x_{ss}^\alpha}$	quasi g.a.s.	quasi g.a.s.	quasi g.a.s.	quasi g.a.s.
zone	$\mathbf{x_{ss}^W}$		l.a.s.		l.a.s.
$W\alpha 1\alpha 2$	$\mathbf{x_{ss}^{\alpha 1}}$	n.a.	l.a.s.	n.a.	l.a.s.
	$\mathbf{x_{ss}^{\alpha 2}}$		unstable (1)		unstable (1)
zone	$\mathbf{x_{ss}^W}$	unstable (1)	unstable (1)	unstable (1)	unstable (1)
$W\alpha 1\beta 1$	$\mathbf{x_{ss}^\alpha}$	unstable (1)	unstable (1)	unstable (1)	unstable (1)
	$\mathbf{x_{ss}^\beta}$	quasi g.a.s.	quasi g.a.s.	quasi g.a.s.	quasi g.a.s.
zone	$\mathbf{x_{ss}^W}$		l.a.s.		l.a.s.
$W\alpha 1\alpha 2\beta 1$	$\mathbf{x_{ss}^{\alpha 1}}$	n.a.	unstable (1)	n.a.	unstable (1)
	$\mathbf{x_{ss}^{\alpha 2}}$		unstable (1)		unstable (1)
	$\mathbf{x_{ss}^\beta}$		l.a.s.		l.a.s.
zone	$\mathbf{x_{ss}^W}$			unstable (1)	
$W\alpha 1\beta 1\beta 2$	$\mathbf{x_{ss}^\alpha}$	n.a.	n.a.	l.a.s.	n.a.
	$\mathbf{x_{ss}^{\beta 1}}$			l.a.s.	
	$\mathbf{x_{ss}^{\beta 2}}$			unstable (1)	
zone	$\mathbf{x_{ss}^W}$		l.a.s.		l.a.s.
$W\alpha 1\alpha 2\beta 1\beta 2$	$\mathbf{x_{ss}^{\alpha 1}}$		unstable (1)		unstable (1)
	$\mathbf{x_{ss}^{\alpha 2}}$	n.a.	unstable (2)	n.a.	unstable (2)
	$\mathbf{x_{ss}^{\beta 1}}$		l.a.s.		l.a.s.
	$\mathbf{x_{ss}^{\beta 2}}$		unstable (1)		unstable (1)
zone	$\mathbf{x_{ss}^W}$				unstable (1)
$W\alpha 1\alpha 2\alpha 3\beta 1$	$\mathbf{x_{ss}^{\alpha 1}}$				unstable (1)
	$\mathbf{x_{ss}^{\alpha 2}}$	n.a.	n.a.	n.a.	unstable (2)
	$\mathbf{x_{ss}^{\alpha 3}}$				unstable (1)
	$\mathbf{x_{ss}^\beta}$				quasi g.a.s.
zone	$\mathbf{x_{ss}^W}$				l.a.s.
$W\beta 1\beta 2$	$\mathbf{x_{ss}^{\beta 1}}$	n.a.	n.a.	n.a.	l.a.s.
	$\mathbf{x_{ss}^{\beta 2}}$				unstable (1)

4.2. Operating diagrams

The criteria for steady states of type α and β to be physical steady states result in operating diagrams with the occurrence of steady states in terms of the process input variables, u_0 and u_1. The operating diagrams for the elementary models I–IV have been discussed extensively by Volcke et al. [19]. Figs. 6–10 display the results for models V–VII.

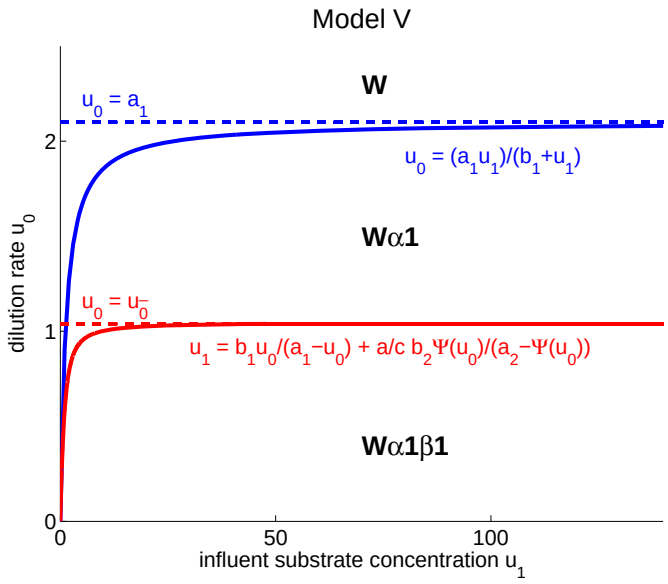

Figure 6: Overall steady state behaviour of model V in terms of u_0 and u_1

The overall steady state behaviour of model V (Fig. 6) is the same as that of models I and II. The corresponding phase trajectories for model V are given in Fig. 7. Up to three steady states can occur, of which only one is (quasi globally) asymptotically stable at a time. For $c_2 \to \infty$, $\Psi(u_0) \to u_0$, and the behaviour of model V is reduced to that of model I, in the same way as the behaviour of model II is reduced to that of model I for $c_1 \to \infty$, implying $\Phi(u_0) \to u_0$.

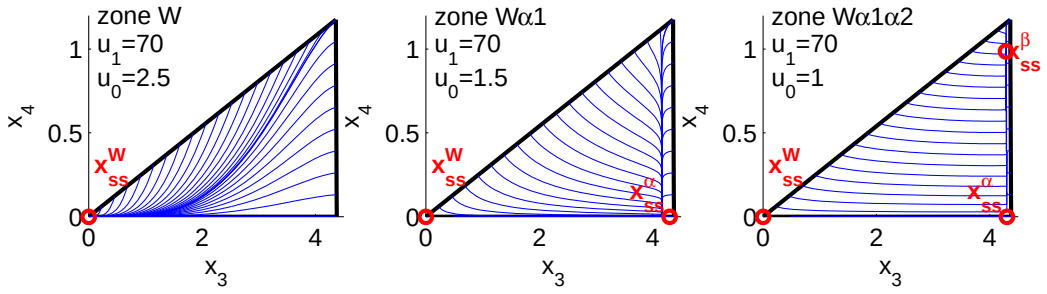

Figure 7: Trajectory fields for model V

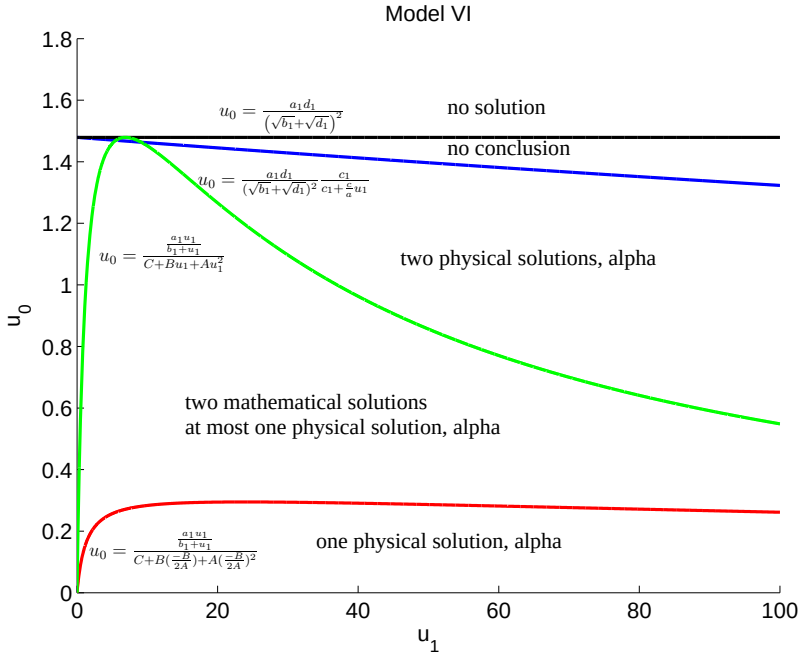

Figure 8: Overall steady state behaviour of model VI in terms of u_0 and u_1

Fig. 8 displays the overall steady state behaviour of model VI. For relatively low values of u_1, corresponding to what is expected in practice for a nitrification process, its steady state behaviour is the same as that of model III. The corresponding phase trajectories are given in Fig. 9. Up to five steady states (operating zone $W\alpha 1\alpha 2\beta 1\beta 2$) can occur, of which two are lo-

cally asymptotically stable (Table 4): $\mathbf{x_{ss}^{W,VI}}$ and $\mathbf{x_{ss}^{\beta 1,VI}}$. In this operating zone, $\mathbf{x_{ss}^{\beta 1,VI}}$ is reached, and product is formed, in case the initial amount of biomass responsible for the first reaction (x_3) in the system is sufficiently high. If this is not the case, the process converges to $\mathbf{x_{ss}^{W,VI}}$, the total washout

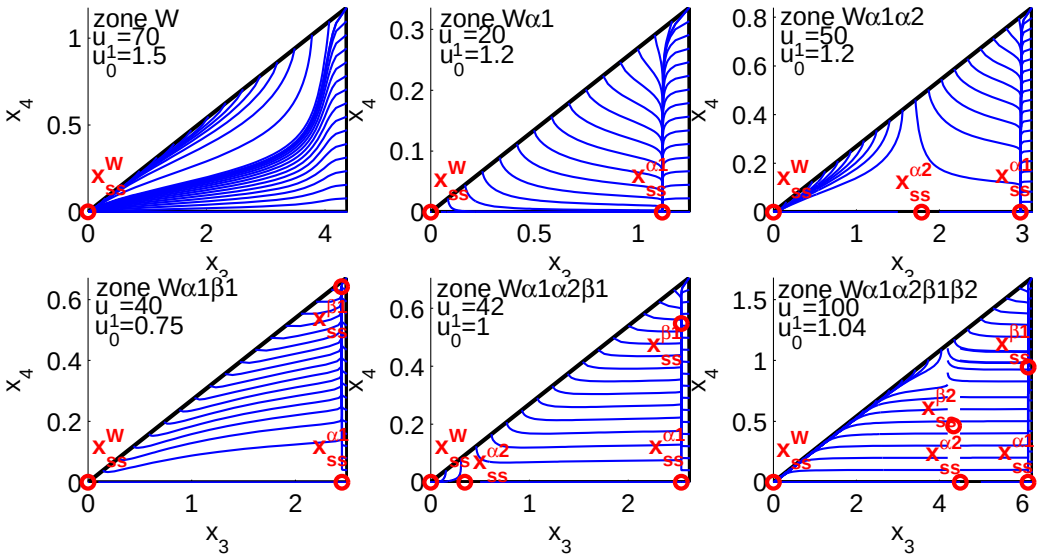

Figure 9: Trajectory fields for model VI

The overall steady state behaviour of Model VII (Fig. 10) is the same as that of model IV. Up to four steady states can occur at the same time (operating zone $W\alpha 1\beta 1\beta 2$), of which two are locally asymptotically stable (Table 4): $\mathbf{x_{ss}^{\alpha 1,VII}}$ and $\mathbf{x_{ss}^{\beta 1,VII}}$. In this operating zone, $\mathbf{x_{ss}^{\alpha 1,VII}}$ is reached, and thus only intermediate is formed, in case the initial amount of biomass responsible for the second reaction (x_4) in the system is sufficiently low. If this is not the case, the process converges to $\mathbf{x_{ss}^{\beta 1,VII}}$, corresponding to product formation.

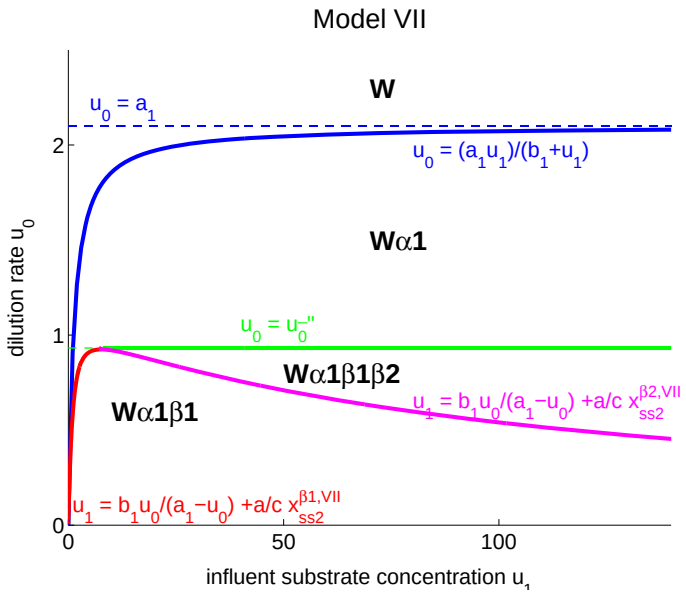

Figure 10: Overall steady state behaviour of model VII in terms of u_0 and u_1

The β-type steady states of model VIII follow from solving two quadratic equations simultaneously. This results in up to 4 steady states if the dilution rate does not exceed the limit defined by (36) and the value of u_1 respects condition (30). The limits (34) and (35) on x_1 and x_2 for obtaining real valued solutions and the conditions $x_1 \geq 0$, $x_2 \geq 0$ define a rectangle in the x_1x_2-plane, where a numerical search algorithm can be used to find all possible steady states. The physical steady states satisfy (28)–(30). However it is not possible to derive curves in the u_0u_1-plane which separate regions with one, two, three or four type β steady states due to the more complicated relationship between the number of steady states and the system's parameters.

5. Conclusions and perspectives

The occurrence of multiple steady states in two-step biological conversion systems has been assessed, considering general kinetic expressions that include substrate limitation and inhibition terms. The calculation of the steady states and their stability analysis has been simplified using a canonical state space model representation. A step-wise procedure has been performed for various models differing in the number of inhibition terms taken up in the reaction rates. Besides the washout state, one or more steady states with only intermediate formation (type α) and product formation (type β) can occur; the exact number depends on the actual kinetic structure. Calculations have been simplified noting that steady states of type α are only dependent on the kinetics of the first reaction step, and taking advantage of the duality between the kinetic expressions for both reactions when assessing the steady states of type β. The overall steady state behaviour of the models has been summarized in terms of the process input variables, in this case the dilution rate and the influent substrate concentration. The resulting diagrams depict operating regions in which certain steady states occur, meaning that they are physical steady states. The stability characteristics of the steady states associated with each operating region have been investigated as well. If some a priori knowledge on microbial kinetics is available, this type of diagrams can be used to define operating conditions which give rise to the desired process behaviour.

The step-wise approach followed in this study has clearly demonstrated the effect of process kinetics on the model behaviour and allowed to gain further insight in the causes of steady state multiplicity. Previous analysis of

a few elementary models [19] indicated that substrate inhibition causes additional steady states (comparing model III or IV with model I), while product inhibition does not affect the number of steady states of the reactor model (comparing model II with model I). Nevertheless, it has now been shown that, in some cases, adding a product inhibition term may indeed further increase the number of steady states (compared to model III, model VI may possess an additional steady state of type α, even though unstable). It is important to realize that the choice of a kinetic structure implies a certain steady state behaviour. Taking into account inhibition effects of multiple components by simply multiplying inhibition terms, a common practice, substantially influences the behaviour of a model, in terms of the number of steady states as well as their stability characteristics. In particular, steady state multiplicity, in the sense that more than one asymptotically stable state occurs and which implies that the steady state behaviour depends on the initial process conditions, will often not be detected when performing simulations.

Finally, the results in this contribution may also serve for experimental design. One can think of setting up experiments to detect the occurrence of different steady states depending on the input variables and, in particular, to identify steady state multiplicity - depending on the initial conditions. It would be most valuable to validate mathematical models on the basis of such experimental findings and to adjust their structure, where necessary.

Acknowledgement

Eveline Volcke is a post-doctoral research fellow of the Research Foundation - Flanders (Belgium) (FWO).

Appendix A. Stability assessment

The stability of the steady states is assessed by determining the eigenvalues of the Jacobian matrix (38). Taking into account the most general kinetic expressions (5)-(6), the partial derivatives in this matrix are calculated as

$$\frac{\partial\, g_3}{\partial\, y_3} = -u_0 + \mu_1(\mathbf{x}) - a\,\eta(\mathbf{x}) + c\,\rho(\mathbf{x}) \tag{A.1}$$

$$\frac{\partial\, g_3}{\partial\, y_4} = -b\,\eta(\mathbf{x}) - d\,\rho(\mathbf{x}) \tag{A.2}$$

$$\frac{\partial\, g_4}{\partial\, y_3} = c\,\xi(\mathbf{x}) - a\,\sigma(\mathbf{x}) \tag{A.3}$$

$$\frac{\partial\, g_4}{\partial\, y_4} = -u_0 + \mu_2(\mathbf{x}) - b\,\sigma(\mathbf{x}) - d\,\xi(\mathbf{x}) \tag{A.4}$$

in which

$$\begin{aligned}\eta(\mathbf{x}) &\triangleq x_3\,\frac{\partial\,\lambda_1}{\partial\, x_1}\\ &= a_1\,c_1\,d_1\,y_3\,\frac{1}{c_1+x_2}\,\frac{b_1\,d_1-(x_1)^2}{(b_1+x_1)^2(d_1+x_1)^2}\end{aligned} \tag{A.5}$$

$$\begin{aligned}\rho(\mathbf{x}) &\triangleq x_3\,\frac{\partial\,\lambda_1}{\partial\, x_2}\\ &= a_1\,c_1\,d_1\,y_3\,\frac{-1}{(c_1+x_2)^2}\,\frac{x_1}{b_1+x_1}\,\frac{1}{d_1+x_1} < 0\end{aligned} \tag{A.6}$$

$$\begin{aligned}\sigma(\mathbf{x}) &\triangleq x_4\,\frac{\partial\,\lambda_2}{\partial\, x_1}\\ &= a_2\,c_2\,d_2\,y_4\,\frac{-1}{(c_2+x_1)^2}\,\frac{x_2}{b_2+x_2}\,\frac{1}{d_2+x_2} < 0\end{aligned} \tag{A.7}$$

$$\begin{aligned}\xi(\mathbf{x}) &\triangleq x_4\,\frac{\partial\,\lambda_2}{\partial\, x_2}\\ &= a_2\,c_2\,d_2\,y_4\,\frac{1}{c_2+x_1}\,\frac{b_2\,d_2-(x_2)^2}{(b_2+x_2)^2(d_2+x_2)^2}\end{aligned} \tag{A.8}$$

The resulting Jacobian matrix is subsequently evaluated in the individual steady states. Table 4 summarizes the resulting stability characteristics. For

the washout state (12), one finds

$$\mathbf{J_{34}}(\mathbf{y_{ss}^W}) = \begin{bmatrix} -u_0 + a_1 \dfrac{u_1}{b_1+u_1}\dfrac{d_1}{d_1+u_1} & 0 \\ 0 & -u_0 \end{bmatrix} \tag{A.9}$$

It is clear that $-u_0 < 0$; the remaining eigenvalue of (A.9) is also strictly negative if and only if

$$u_0 > a_1 \frac{u_1}{b_1+u_1}\frac{d_1}{d_1+u_1} \tag{A.10}$$

Condition (A.10) is fulfilled in the operating region W in which the washout state ($\mathbf{x_{ss}^W}$) is the only steady state, as well as in the operating regions $W\alpha 1\alpha 2$, $W\alpha 1\alpha 2\beta 1$ and $W\alpha 1\alpha 2\beta 1\beta 2$, for which two steady states of type α occur at the same time. Under this condition, the steady state ($\mathbf{x_{ss}^W}$) is asymptotically stable.

For steady states of type α, satisfying (13), the Jacobian matrix (38) becomes

$$\mathbf{J_{34}}(\mathbf{y_{ss}^\alpha}) = \begin{bmatrix} -a\,\eta(\mathbf{x_{ss}^\alpha}) + c\,\rho(\mathbf{x_{ss}^\alpha}) & \left.\dfrac{\partial\, g_3}{\partial\, y_4}\right|_{\mathbf{y=y_{ss}^\alpha}} \\ 0 & -u_0 + \mu_2(\mathbf{x_{ss}^\alpha}) \end{bmatrix} \tag{A.11}$$

A steady state $\mathbf{x_{ss}^{\alpha i}}$ $(i = 1, 2)$ is asymptotically stable if the eigenvalues of the matrix (A.11) are all strictly negative:

$$-a\,\eta(\mathbf{x_{ss}^\alpha i}) + c\,\rho(\mathbf{x_{ss}^\alpha i}) < 0 \tag{A.12}$$

$$u_0 > \mu_2(\mathbf{x_{ss}^\alpha i}) \tag{A.13}$$

The Jacobian matrix for steady states of type β, determined by (15), is found as

$$\mathbf{J_{34}}(\mathbf{y_{ss}^\beta}) = \begin{bmatrix} -a\,\eta(\mathbf{x_{ss}^\beta}) + c\,\rho(\mathbf{x_{ss}^\beta}) & -b\,\eta(\mathbf{x_{ss}^\beta}) - d\,\rho(\mathbf{x_{ss}^\beta}) \\ c\,\xi(\mathbf{x_{ss}^\beta}) - a\,\sigma(\mathbf{x_{ss}^\beta}) & -b\,\sigma(\mathbf{x_{ss}^\beta}) - d\,\xi(\mathbf{x_{ss}^\beta}) \end{bmatrix} \tag{A.14}$$

References

[1] P. Agrawal, C. Lee, H.C. Lim, D. Ramkrishna, Theoretical investigations of dynamic behavior of isothermal continuous stirred tank biological reactors, Chem. Eng. Sci. 37(3) (1982) 453-462.

[2] G. Bastin, D. Dochain, On-line Estimation and Adaptive Control of Bioreactors, Elsevier, Amsterdam, 1990.

[3] O. Bernard, Z. Hadj-Sadok, D. Dochain, A. Genovesi, J.P. Steyer, Dynamical model development and parameter identification for an anaerobic wastewater treatment process, Biotechnol. Bioeng. 75(4) (2001) 424-438.

[4] H. Chiang, M. Hirsch, F.Wu, Stability regions of nonlinear autonomous dynamical systems, IEEE Trans. Automat. Control 33 (1988) 1627.

[5] J. Guckenheimer, P. Holmes, Nonlinear Oscillations, Dynamical Systems and Bifurcations of Vector Fields, Springer, New York, 1983.

[6] X.M. Guo, E. Trably, E. Latrille, H. Carrre, J.P. Steyer, Hydrogen production from agricultural waste by dark fermentation: a review, International Journal of Hydrogen Energy, in press.

[7] M. Hajji, F. Mazenc, J. Harmand, A mathematical study of a syntrophic relationship of a model of anaerobic digestion process, Math. Biosci. Eng. 7(3) (2010) 641-656.

[8] J. Hess, O. Bernard, Design and study of a risk management criterion for

an unstable anaerobic wastewater treatment process, J. Process Control 18(1) (2008) 71-79.

[9] M. Sbarciog, E.I.P. Volcke, M. Loccufier, E. Noldus, Stability boundaries of a SHARON bioreactor model with multiple equilibrium points, Nonlinear Dyn. Syst. Theory 6(2) (2006) 191-203.

[10] M. Sbarciog, M. Loccufier, E. Noldus, The computation of stability boundaries in state space for a class of biochemical engineering systems, J. Comput. Appl. Math. 215(2) (2008) 557-567.

[11] M. Sbarciog, The Stability of Biochemical Reaction Systems, PhD thesis, Ghent, 2008.

[12] M. Sheintuch, Dynamics of commensalistic systems with self- and cross-inhibition, Biotechnol. Bioeng. (1980) 2557-2577.

[13] M. Sheintuch, B. Tartakovsky, N. Narkis, M. Rebhun, Substrate inhibition and multiple states in a continuous nitrification process, Water Res. 29(3) (1995) 953-963.

[14] S. Shen, G.C. Premier, A. Guwy, R. Dinsdale, Bifurcation and stability analysis of an anaerobic digestion model, Nonlinear Dyn. 48 (2007) 391-408.

[15] G. Sin, D. Kaelin, M.J. Kampschreur, I. Takacs, B. Wett, K.V. Gernaey, L. Rieger, H. Siegrist, M.C.M. van Loosdrecht, Modelling nitrite in wastewater treatment systems: a discussion of different modelling concepts, Water Sci. Technol. 58(6) (2008) 1155-1171.

[16] H.L. Smith and P. Waltman, The Theory of the Chemostat, Dynamics of Microbial Competition, Cambridge Studies in Mathematical Biology, Vol. 13, Cambridge University Press, Cambridge, London, 1995.

[17] C.C. Tong, L.S. Fan, Concentration multiplicity in a draft tube fluidized-bed bioreactor involving two limiting substrates, Biotechnol. Bioeng. 31 (1988) 24-34.

[18] M.C.M. van Loosdrecht, S. Salem, Biological treatment of sludge digester liquids, Water Sci. Technol. 53(12) (2006) 11-20.

[19] E.I.P. Volcke, M. Sbarciog, M. Loccufier, P.A. Vanrolleghem, E.J.L. Noldus, Influence of microbial growth kinetics on steady state multiplicity and stability of a two-step nitrification (SHARON) model, Biotechnol. Bioeng. 98(4) (2007) 882-893.